Journal of Hazardous Materials 181 (2010) 692–699

Contents lists available at ScienceDirect

Journal of Hazardous Materials

journal homepage: www.elsevier.com/locate/jhazmat

Removal of rotenone insecticide by adsorption onto chemically modified activated carbons

Anissa Dhaouadi, Lotfi Monser, Nafaâ Adhoum*

Laboratoire de Chimie Analytique et d'Electrochimie, Institut National des Sciences Appliquées et de Technologie, Centre Urbain Nord B.P.N 676, 1080 Tunis Cedex, Tunisia

ARTICLE INFO

Article history:
Received 30 December 2009
Received in revised form 3 May 2010
Accepted 17 May 2010
Available online 9 June 2010

Keywords:
Activated carbon
Adsorption isotherm
kinetic
Surface chemistry
Rotenone

ABSTRACT

The removal of rotenone from synthetic and real wastewaters using modified activated carbons has been investigated. In order to enhance the removal capacity of rotenone, activated carbon was chemically modified through impregnation with NH_3 and $(NH_4)_2S_2O_8$ solutions. The resulting carbons were found to present different surface chemistries, while possessing similar textural properties. The adsorption data obtained at 298 K, on plain and modified carbons were well represented by the Langmuir isotherm model ($R^2 > 0.997$). The highest adsorption capacity ($Q_m = 270.3\ mg\ g^{-1}$) was obtained with the ammonia-treated activated carbon. The relative effect of different surface groups on adsorption capacities were found to be in accordance with the $\pi - \pi$ dispersive interaction model. The adsorption kinetic models have provided useful insights into rotenone adsorption mechanism. It was concluded that rotenone sorption process followed pseudo-second order model and was controlled by intra-particle diffusion mechanism with a significant contribution of film diffusion. The successful adsorptive removal of rotenone, from real wastewater samples on fixed bed columns, have demonstrated the suitability of this method as an effective alternative solution for the treatment of contaminated wastewaters.

1. Introduction

Pesticide contamination of ground water and surface water has been recognised as widespread and significant water quality concern [1,2]. Pesticide-containing wastewaters have been mainly generated from applicators container rinsates, agrochemical industries, formulating and manufacturing plants [2,3]. Improper disposal of these wastes may increase the risk of contamination of the aqueous environment causing detrimental ecological and human health consequences. Among various cleanup technologies, the adsorption on activated carbon (AC) is one of the well-established and effective techniques [4–6]. AC adsorbents are now widely employed for product purification and wastewater treatment, because of their exceptionally large surface areas, well-developed internal pore structure as well as their surface reactivity attributed to the existence of a wide spectrum of oxygen-containing surface groups [7–12]. Being mechanically robust and highly hydrophobic, molecules with large hydrophobic groups can be strongly adsorbed onto carbon surface. The major drawback of adsorption methods is their environmentally incomplete character because they only transfer but not degrade pollutants. In this case, the used adsorbent becomes a hazardous material demanding further treatment subsequently. Nevertheless, some interesting options based on the application of advanced oxidation methods, are under development and may constitute in the near future an efficient solution to degrade the adsorbed contaminants and regenerate the activated carbon on-site and in-situ [13]. Several works [14] emphasized the key role of surface chemistry in adsorption of organic solutes from aqueous phase and concluded that adsorptive properties of AC are mainly determined by its chemical composition. It is well known that adsorption behaviour is decisively influenced by surface oxygen complex content, which determines the charge of the surface, its hydrophobicity and the electronic density of the graphene layers. To increase the concentration of surface oxygen groups a wide range of oxidizing or/and acid agents such as HNO_3, H_2O_2, $HClO_4$, $(NH_4)_2S_2O_8$, O_3 have been successfully applied [15–16]. The introduction of acid surface groups was always accompanied by an important destruction of the basic sites excepting for $(NH_4)_2SO_4$ and H_2O_2. Possibly, H_2O_2 was capable to introduce some recognised basic groups as quinones, chromenes or pyrones due to its rather soft oxidation strength. In contrast, surface oxides can be reduced by treatment with alkaline or reductants solutions, e.g., NH_3, NaOH, $NaHSO_3$, etc. [17–18]. In general, several research groups have recorded significant decrease in the adsorption of organic compounds such as dodecanoic acid [19], methyl isoborneol [20] and phenol [21] upon increasing the oxygen content of the carbon adsorbent (mainly by surface oxidation). In addition, the elimination of acidic oxygen-containing groups from

* Corresponding author. Tel.: +216 1 703627; fax: +216 1 704329 1.
E-mail address: Nafaa.adhoum@insat.rnu.tn (N. Adhoum).

0304-3894/$ – see front matter © 2010 Elsevier B.V. All rights reserved.
doi:10.1016/j.jhazmat.2010.05.068

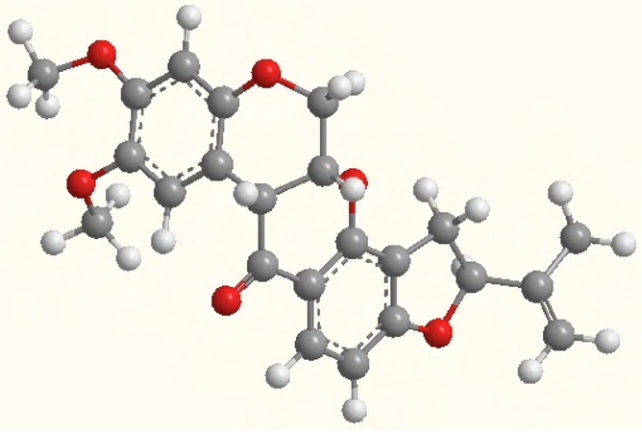

Scheme 1. Chemical structures of Rotenone (molecular surface = 141.4 10^{-20} m^2).

activated carbons was found to increase adsorption of phenols [22]. This prompted us to investigate the adsorption of rotenone, a sparingly soluble insecticide, on plain and modified activated carbons exposed to different pre-treatments, in an attempt to clarify and supply additional information on the effect of surface chemistry.

Rotenone is a broad-spectrum, non systemic botanical insecticide derived from the roots and bark of Derris, Tephrosia, Amorpha and Lonchocarpus, tropical plant species [23]. It is mainly employed as a household insecticide and as a tool for eradicating nuisance fish populations in lake and enclosed waters [24,25]. This compound is a well-characterized specific inhibitor of NADH/ubiquinone (complex I) of the mitochondrial electron transport chain [26]. Several studies have shown that rotenone crosses cellular membranes freely and impairs oxidative phosphorylation, leading to cytochrome C release, followed by DNA fragmentation and cell death [27]. It is believed to contribute to the genesis of promyelocytic leukemias [28] and neuroblastomas [29]. On the other hand, administration of rotenone has been shown to produce selective nigrostriatal dopaminergic neurodegeneration [25,30–31] which leads to anatomical and behavioural symptoms resembling Parkinson's disease [31–33]. Nowadays, rotenone is used in Europe with strong restrictions regarding its environmental hazards [34]. Once deposited on soils or in enclosed waters, rotenone undergoes thermo and photo-chemical degradation induced by sunlight [34]. In the last years, the studies on rotenone degradation have been limited to investigating natural photochemical behaviour in liquid phase [35–36] and in soils [34]. Lacking of scientific data related to the toxicity of photo-degradation products associated with the spectacular growth of organic agriculture, leading to a massive use of botanical insecticides; make it necessary and important to find effective low-cost and environmentally clean methods of treating rinsates and waste products

The primary goal of the current study was to investigate the adsorption behaviour of rotenone onto activated carbon adsorbents with different surface oxygen complex contents in an effort to seek an effective remediation technology of contaminated wastewaters. A second goal was to obtain a better understanding of the mechanism of rotenone adsorption onto these ACs by clarifying the roles of adsorbent porosity and surface chemistry.

2. Experimental

2.1. Chemicals and materials

All chemicals and organic solvents were obtained in analytical-reagent grade and used without further purification. Rotenone (Scheme 1) and methanol were purchased from (Fluka, France). Since rotenone is sparingly soluble in water, a stock solution containing 1000 mg L^{-1} was prepared in methanol-water mixture (10:90). All subsequent solutions were freshly prepared using doubly distilled ultra-pure water and methanol mixture.

The activated carbon used in the present investigation was obtained from Panreac (France) with a particle size of 100-150 μm and a specific surface area, as measured by the BET method, of 986 m^2 g^{-1}. The original carbon was conditioned by boiling in deionised water to remove fines and residual physically adsorbed chemicals. Then the washed carbon was oven dried in thin layers at 110 °C for 24 h and kept in desiccator for use.

2.2. Preparation and characterisation of activated carbon

Two chemical modification procedures were applied to the virgin carbon in order to investigate the effect of surface chemistry on the adsorption behaviour. The first pre-treatment involved liquid oxidation with ammonium persulfate, by submerging the virgin carbon in (2 M) $(NH_4)_2S_2O_8$ at 25 °C for 2 hours. The obtained sample is referred to as (AC-P). The second pre-treatment was carried out by submerging virgin carbon in (2 M) ammonia solution at 25 °C for 2 hours. The resultant sample is labelled as (AC-A). After completion of the pre-treatments, all samples were thoroughly washed with distilled water and oven dried in the same manner as the original carbon.

Various characterization methods have been used to determine physicochemical properties of virgin and modified activated carbons. Surface areas and pore volumes of the ACs were evaluated from low temperature (77 K) nitrogen adsorption isotherms, using a computer controlled gas sorption analyser (ASAP 2000). Samples were degassed overnight at 300 K prior to the adsorption analysis. The surface area, S_{N2}, was calculated by applying the BET equation to the corresponding isotherms. Pore size distributions were obtained from the combination of two widely accepted models: the DFT for the micropores (<20 Å) and the BJH theory for meso- and macro-pore volumes [37].

Surface functional groups were determined by standard neutralization-titration with HCl, NaOH, Na_2CO_3, $NaHCO_3$ (0.05 N in water) according to the Boehm procedure [4,38]. The number and type of acid groups were calculated by considering that the difference between NaOH and Na_2CO_3 consumption corresponds to the weakly acidic phenolic groups, while difference between Na_2CO_3 and $NaHCO_3$ consumption corresponds to the lactonic groups. Carboxylic groups were therefore quantified by direct titration with $NaHCO_3$. On the other hand, total basic sites were evaluated by titration with HCl.

The pH of the point of zero charge (pH_{PZC}), i.e. the pH above which the total surface of the carbon particles is negatively charged, was measured by the so-called pH drift method [39–41]. Accurately weighed portions of each carbon (0.1 g) were filled into 50 mL conical flasks containing 25 mL of 0.1 M NaCl standard solutions. The initial pH's of these solutions were varied (pH 2-12) and then shaken mechanically for 48 hours. Initial pH were adjusted by adding either HCl or NaOH (0.2 M) and the ionic strength was kept constant (I = 0.1). After a period of 48 hours shaking, the final pH values of the suspensions were determined using a Mettler-Toledo 340 pH-meter. The final pH values were plotted against the initial pH values and the pH at which the curve crosses the line pH(final) = pH(initial) is taken as the pH_{PZC} of the given carbon.

2.3. Analytical methods

The rotenone concentration was analyzed by HPLC system (Beckman Instruments Inc., USA) consisting of an isocratic LC pump, a Rheodyne injection valve (20 μL) and a diode array detector. The separation was achieved on a Supelcosil LC18 column (250 mm,

Table 1
Selected physicochemical properties of the parent and modified carbon samples.

Activated carbon	S_{BET} ($m^2\ g^{-1}$)	S_{micro} ($m^2\ g^{-1}$)	V_{micro} ($cm^3\ g^{-1}$)	V_{meso} ($cm^3\ g^{-1}$)	V_{macro} ($cm^3\ g^{-1}$)	Mean pore diameter (nm)	pH_{pzc}	Surface functional groups (mmol g^{-1})			
								Carboxylic	Lactone	Phenolic	Basic
AC	986	570	0.326	0.462	0.092	1,93	5.4	0.15	0.25	0.05	0.25
AC-A	1004	594	0.338	0.454	0.088	1.91	6.5	0.05	0.25	0.05	0.50
AC-P	902	534	0.306	0.476	0.011	1.96	3.8	0.45	1.3	0.35	0.05

4.6 mm i.d., 5 μm particle size). The mobile phase consisted of 90% acetonitrile and 10%water delivered at a flow rate of 1 mL min^{-1}. The detection wavelength of rotenone was set at 276 nm.

2.4. Sorption kinetics

In order to determine the kinetics of the sorption process, an accurately weighed mass portions of plain or modified activated carbon (0.1 g) were introduced into a 250 mL flask containing methanol-water solution (10:90 v/v). Appropriate amounts of rotenone stock solution (1000 mg L^{-1}) were added to each flask to achieve the required concentrations. Samples were agitated on a horizontal shaker and the concentration of freely dissolved rotenone was determined at different time intervals using HPLC technique.

2.5. Batch adsorption experiments

Adsorption experiments of rotenone on activated carbon were carried out using a batch method. Portions of 0.1 g activated carbon were added to 100 mL Erlenmeyer flasks, containing 100 mL of rotenone solutions (from 20 to 300 mg L^{-1}). These solutions were shaken for 24 hours, using a thermostated horizontal shaker (T = 25 °C). The time needed to reach equilibrium was determined from kinetic experiments. Upon completion of experiments, samples of supernatant was taken from each flask and filtered through a 0.45 μm syringe filter. The filtrate obtained was then analyzed by HPLC to determine the equilibrium concentration of dissolved rotenone. The equilibrium-amounts adsorbed onto ACs were calculated using a mass balance analysis.

2.6. Procedure of column packing

Three samples of plain and modified activated carbons (2.5 g each) were packed into glass columns (200 mm height, 20 mm i.d.). These columns were used for rotenone removal from a real rinsate water received from agricultural application equipment. Chemical oxygen demand (COD) of the real sample was found to be 180 mg L^{-1} with 39 mg L^{-1} rotenone content. The wastewater samples were introduced through the columns and the effluent concentrations were analyzed. The flow rates for the three columns were maintained at 2 mL min^{-1} with a contact time of about 8 min.

3. Results and discussion

3.1. Surface chemistry

Physicochemical characterisation of virgin and modified activated carbons, are shown in Table 1. These results show that the studied samples have quiet similar BET surface areas (ranging from 898 to 1004 $m^2\ g^{-1}$) and pore size distributions. It is observed that treatment with $(NH_4)_2S_2O_8$ caused less than 9% loss of the surface area, attributable to partial pore structure deterioration of the carbon during the pre-treatment. On the other hand, ammonia treatment does not significantly change the surface area within the experimental error of BET determinations. In addition, comparing the studied samples porosities, it can be observed that no significant changes (less than 6%) in the porous structure was recorded following applied treatments. Thus it can be concluded that the applied chemical modifications caused only slight changes in the textural properties. In contrast, the surface chemical structures of plain and modified ACs were highly diverse. Functional groups concentrations determined from Boehm's titration method are shown in Table 1. As expected, these results provide an evidence on the dramatic increase of total acidic sites upon $(NH_4)_2S_2O_8$ oxidation. The acidic groups of AC-P are five times higher than that of untreated AC. This behaviour is attributed to generation of new oxygen functionalities during $(NH_4)_2S_2O_8$ oxidation [42]. On the other hand, ammonia treatment led to a significant enhancement of basic surface groups, which are measured to be almost two-fold higher than on virgin carbon. Taking into account the mild conditions used during ammonia treatment, the obtained results could be mainly ascribed to neutralization of acidic surface groups rather than incorporation of nitrogen structures in the carbon matrix. The treatment with $(NH_4)_2S_2O_8$, mostly generates lactonic groups, although concomitant increases in carboxylic and phenolic groups are recorded. These results contrast with that published by Santiago et al. [15] reporting that $(NH_4)_2S_2O_8$ treatment mostly generates phenolic groups. We have not a clear explanation to this contradiction, but it could be attributed to the higher surface density of carboxylic groups present on plain AC, used in this study, which suggests their possible condensation with phenolic groups to form lactones [15,43]. The modification with ammonia drastically reduces the concentration of carboxylic groups, while phenolic and lactonic groups are not affected.

The comparative results of pH_{PZC} for plain and modified carbons are also shown in Table 1. It is apparent from these results that $(NH_4)_2S_2O_8$ treatment of AC induced a significant decrease of (PZC), while the opposite evolution is observed after ammonia-treatment. This is consistent with the above discussed changes of surface functional groups. As expected, the pH_{PZC} decreases upon increasing the total acidic sites number and increases with increasing basic surface groups.

3.2. Rotenone adsorption studies

Knowledge of adsorption isotherm is not only important to understand the mechanism of interaction between carbon surface and adsorptives, but it is also critical in optimizing the use of carbon as adsorber. Rotenone adsorption isotherms on AC, AC-P and AC-A at room temperature (25 °C) are depicted on Fig. 1. The general shape of the presented isotherms suggests that all studied carbons have a high affinity for rotenone, as evidenced from the large amount adsorbed at low equilibrium solution concentration. The second important feature of the presented isotherms is the presence of a strongly marked plateau at higher adsorptive concentrations suggesting that they are of the I-type, following IUPAC classification. Such behaviour is typical of the Langmuir isotherm. The experimental adsorption data were adjusted to two famous two-parameter isotherm equations: the Langmuir and Freundlich models, in order to interpret and analyze the adsorption process.

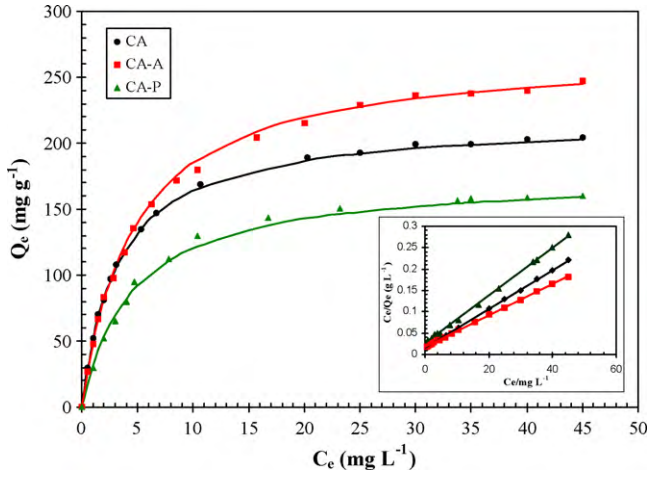

Figure 1. Adsorption isotherm of rotenone on plain and modified activated carbons at T = 25 °C. The inset shows correlation of experimental data to Langmuir isotherm model.

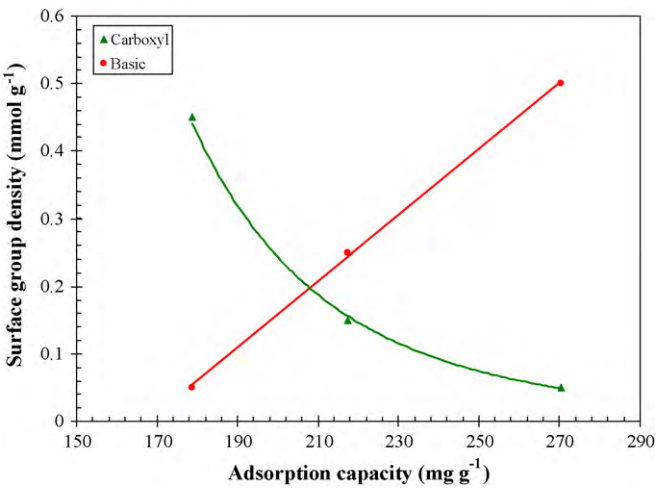

Figure 2. Correlation of the maximum adsorption capacities of rotenone with carboxyl and total basic group densities.

The Langmuir isotherm is mainly used to describe monolayer adsorption process [44–45] and is generally used in its linear form as follows:

$$\frac{C_e}{Q_e} = \frac{1}{Q_m K_L} + \frac{C_e}{Q_m} \quad (1)$$

Where Q_e is the amount of solute adsorbed per unit mass of adsorbent ($mg\,g^{-1}$), C_e is the equilibrium concentration of solute in solution ($mg\,L^{-1}$). The parameter Q_m($mg\,g^{-1}$) corresponds to the total monolayer coverage and K_L($L\,mg^{-1}$) is the Langmuir equilibrium constant which can be considered a measure of the free energy of adsorption.

On the other hand, Freundlich model describes satisfactorily adsorption on surfaces with non-uniform energy distribution, assuming that surface sites of higher affinity are occupied first and that the binding strength decreases upon increasing the degree of site occupation [46]. The linear form of the Freundlich equation is given by the following equation:

$$Ln(Q_e) = \frac{1}{n} Ln(C_e) + Ln(K_F) \quad (2)$$

Where K_F($L^{1/n}\,mg^{-1/n}$) is the adsorption constant related to sorption capacity and n is characteristic constant related to sorption intensity of the adsorbent [44].

The isotherm parameters were evaluated by a non-linear least square method and the best isotherm model was that which has the highest regression coefficient. Modelling results and estimated parameters values for each model are shown in Table 2. As can be seen, experimental results of rotenone adsorption on plain and modified carbons are adjusted better to the Langmuir isotherm with regression coefficients higher than 0.999. It is observed from the maximum adsorption capacities (Q_m) that rotenone uptake was clearly enhanced by ammonia treatment and significantly reduced by $(NH_4)_2S_2O_8$ oxidative treatment. Maximum adsorption capacities of rotenone onto AC-A and AC-P were (24.3%) higher and (17.8%) lower, respectively than that measured with plain carbon. Taking into account the slight effect of applied treatments on textural parameters, it could be concluded that the observed differences in adsorption behaviour of rotenone on plain and modified carbons have to be mainly ascribed to differences between their surface chemistry.

The detailed analysis of adsorption data with respect to surface chemistry leads to the observation that carboxyl and the basic groups play the most important role in rotenone adsorption. Fig. 2 shows that a highly significant correlation exists between rotenone adsorption capacity and the total concentration of surface bases and carboxyl groups. In contrast, there is no obvious correlation between the amount of rotenone adsorbed and phenolic or lactonic surface group densities. These observations are similar to those reported by Terzyk [21] for phenol adsorption on AC. The above reported behaviour is consistent with the well established fact that incorporation of acidic surface oxygen-containing groups, that withdraw electrons from the graphene layers, should lead to weaker dispersive interactions between the adsorptive aromatic ring and the π electron system of carbon basal planes and consequently decreases the number of adsorption sites [21,47]. By the same reasons, decreasing oxygen-containing groups and incorporation of nitrogen basic groups would increase the π electron density of the graphene layers and enhance rotenone adsorption as observed for AC-A. On the other hand it is worth noting to mention that the maximum adsorption capacities of rotenone on the studied carbons (between 178.6 and 270.3 $mg\,g^{-1}$ i.e. 452.9 and 685.5 $\mu mol\,g^{-1}$) are higher than that of total basic surface groups reported in Table 1 (between 50 and 500 $\mu mol\,g^{-1}$). This suggests that the donor-acceptor argument, assuming the formation of donor-acceptor complexes between the surface carboxyl groups, acting as electron donors, and the aromatic ring acting as the acceptor [49], is quite unlikely for rotenone adsorption on both plain and modified carbons. Thus it can be concluded that the mechanism of rotenone adsorption is based mainly on the pi-pi dispersive interaction [48], excluding by the way the donor acceptor mechanism because of the lack of adsorption sites. This conclu-

Table 2
Langmuir and Freundlich equilibrium isotherm parameters for the adsorption of rotenone onto various adsorbents.

Activated carbon	Langmuir			Freundlich		
	K_L($L\,mg^{-1}$)	Q_m($mg\,g^{-1}$)	R^2	K_F($mg\,g^{-1}$)	n	R^2
AC	0.311	217.4	0.999	56.15	2.32	0.922
AC-A	0.208	270.3	0.999	52.51	1.99	0.924
AC-P	0.220	178.6	0.998	38.47	2.17	0.946

sion is similar to that reached by several authors [47,49–50] for the adsorption of phenol, nitrobenzene and nitrophenol. In addition, Table 2 shows that ammonia treatment gives lower Langmuir equilibrium constant (K_L) when compared to the plain carbon, reflecting a weaker adsorption of rotenone on AC-A, in spite of its higher adsorption capacity. A possible explanation may be, at least partially, attributed to an increase of competitive water adsorption onto protonated surface basic sites, leading to a weaker binding energy between carbon and rotenone. This explanation points out the possible role of water adsorption on changing the energy of solute-adsorbent interaction.

3.3. Kinetic of Rotenone adsorption

In order to gain a further understanding of rotenone adsorption mechanism and to shed light onto the rate determining steps that control the adsorption rate, rotenone adsorption kinetics on plain and modified carbons have been monitored and analysed.

Sorption kinetic results of rotenone, presented in terms of solid phase accumulation versus time, at different initial concentrations are shown in Fig. 3-A. As can be seen, the kinetic trends were quite similar for plain and modified carbons. It appears that the sorption rate is high at the initial period and typically 80 to 85% of the ultimate adsorption occurs during the first hour of contact. Subsequently the process slowed down gradually until it attained an equilibrium beyond which there was no significant increase in the rate of removal. From these results, it is also clear that the insecticide adsorption rate increases upon increasing the initial concentration. This behavior is expected since a higher concentration gradient, existing between the solution and the adsorbent phase, is promoted by an increased initial concentration of rotenone. Three kinetic models: pseudo-first order, pseudo-second order and Elovich equation, were used to fit the experimental data. However, neither Elovich nor the pseudo-first order model could fit adequately the adsorption of rotenone over the entire evaluated treatment period. Only the pseudo-second order model provided a very good simulation of the experimental data at all investigated conditions. This was evidenced by the high linearity of the plot $\frac{t}{Q_e}$ against time (Fig. 3-B) giving the best regression coefficients for this work ($r^2 > 0.998$). The pseudo-second order rate constant (k_2) and the amount of adsorbed insecticide (Q_e), obtained from the intercept and slope of the plot of $\frac{t}{Q_e}$ vs. t, as well as the regression coefficients are listed in Table 3. These results seem to indicate a slightly slower adsorption rate of rotenone on AC-A, when compared to AC and AC-P samples. To confirm this observation and to identify the slowest step that governs the adsorption process, a closer look at the kinetic adsorption data is required.

In general, adsorption rate from liquid solution depends on the rate of the different steps involved in the mechanism. Nevertheless, considering that adsorption stage is usually expected to be very rapid and does not represent the rate determining step, only external and intra-particle diffusion throughout the micro-porous network of the adsorbent will determine the adsorption rate.

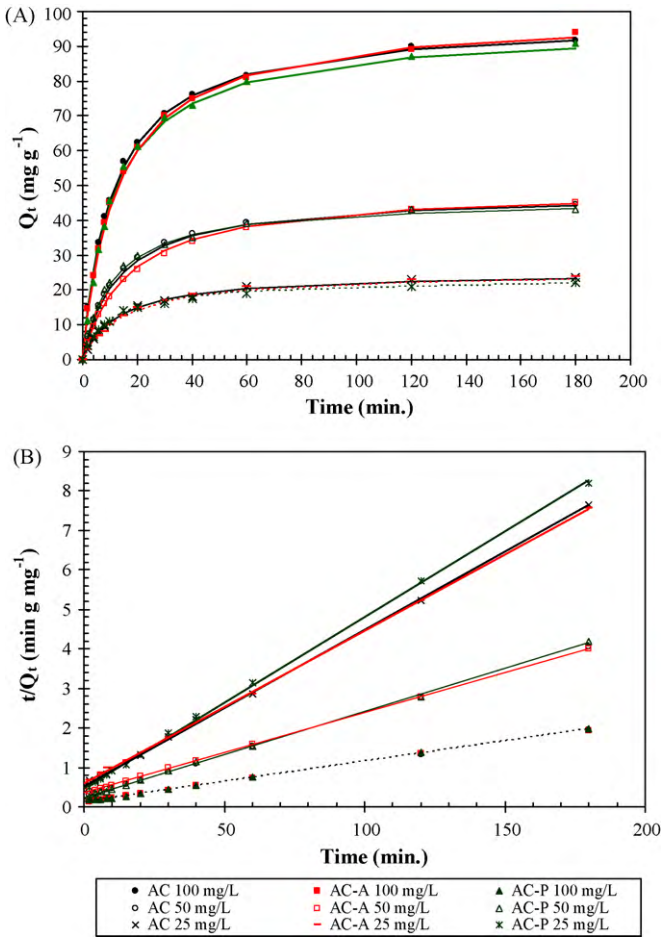

Figure 3. (A) Sorption kinetics of rotenone at different concentrations on plain and modified carbons. (B) Plots of pseudo-second-order kinetic model for data of Fig. 3A. T = 25 °C.

To distinguish between external and intra-particle diffusion and to test whether this later process is the rate limiting step, kinetic data were analyzed using the Weber and Morris model [51]. According to this theory, the following empirical equation should hold, under conditions where intra-particle diffusion is involved:

$$Q_t = k_{ip}\sqrt{t} + C \quad (3)$$

Where k_{ip} (mg g^{-1} min$^{-1/2}$) is the intra-particle diffusion rate constant and C (mg g^{-1}) is a constant that gives idea about the thickness of boundary layer.

Thus to check the equation with experimental data, the values of Q_t are plotted against $\sqrt{t}$. A straight line should be obtained if the intra-particle diffusion is involved in the adsorption process. More-

Table 3
Kinetic constants for rotenone adsorption on plain and modified carbons.

Activated carbon	Initial concentration (mg L^{-1})	Q_e (mg g^{-1}) (experimental)	Q_e (mg g^{-1}) (calculated)	k_2 (g mg^{-1} min^{-1})	R^2
AC	100	95.5	94.5	8.87 x 10^{-4}	0.999
	50	45.9	45.8	1.56 x 10^{-3}	0.998
	25	24.2	24.1	3.09 x 10^{-3}	0.999
AC-A	100	97.1	97.8	7.72 x 10^{-4}	0.997
	50	47.2	47.8	1.21 x 10^{-3}	0.994
	25	24.7	24.9	2.62 x 10^{-3}	0.999
AC-P	100	93	92.2	8.97 x 10^{-4}	0.997
	50	45.1	44.6	1.91 x 10^{-3}	0.996
	25	22	21.7	4.05 x 10^{-3}	0.999

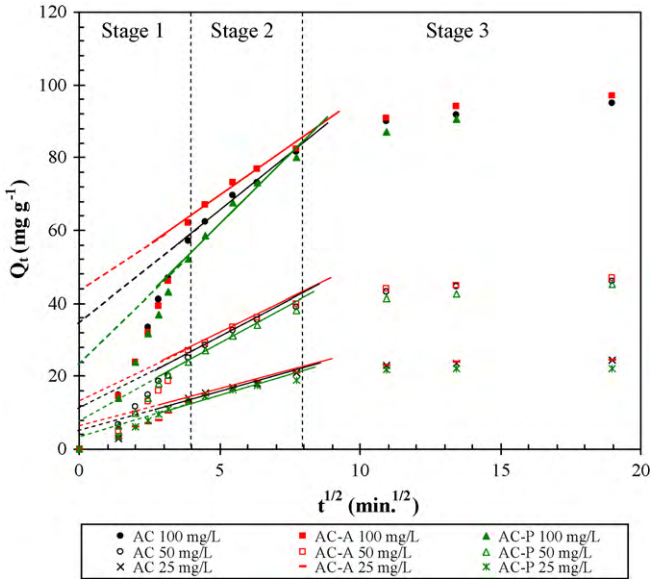

Figure 4. Plots of intraparticle diffusion model for adsorption of rotenone, at different initial concentrations, onto plain and modified activated carbons. T = 25 °C.

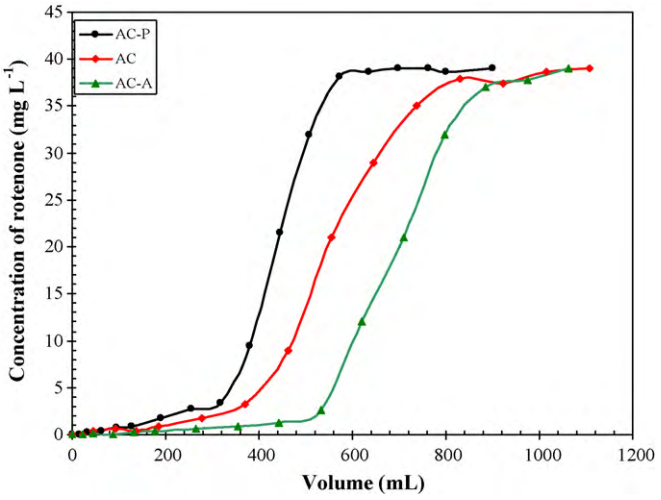

Figure 5. Breakthrough curves of rotenone onto plain (AC), ammonia-impregnated (AC-A) and persulfate-impregnated (AC-P) carbon columns. wastewater contained 39 mg L^{-1} of rotenone.

over, if this line passes through the origin, then the rate controlling step is solely due to the internal diffusion.

The Weber-Morris plots for rotenone adsorption on plain and modified carbons, at different initial concentrations (Fig. 4) have the same general features of an initial curved portion followed by a linear portion and a plateau. The initial curved portion may be attributed to the boundary layer diffusion stage (liquid-film mass transfer). The second linear portion may be attributed to intra-particle diffusion stage, while the plateau corresponds to the final equilibrium stage [45]. It is apparent from the graphs that the straight lines of the second stage do not pass through the origin. This indicates that intra-particle diffusion is involved in the adsorption process but it is not the only rate-limiting mechanism and that some other mechanisms are involved which may also simultaneously control the rate of rotenone adsorption. The calculated values of (k_{ip}) and (C), as obtained from the slope and the intercept of straight lines are given in Table 4. The intra-particle rate constants were found to increase in the following order AC-A < AC < AC-P, suggesting a faster (respectively slower) internal diffusion of rotenone within AC-P (respectively AC-A) porosity, when compared to AC sample. These differences in internal diffusion rate may be, most probably, ascribed to changes in surface chemistry. Several authors presumed that at high dilution and neutral pH, the positive surface charge resulting from the protonation of the strongest surface bases, leads to the increase in water adsorption originating clusters that may block micropores entrance and prevent the access of adsorptive molecules to adsorption sites [50,52,53]. Taking this into consideration, it could be assumed that competitive adsorption of water, enhanced by the basic character of AC-A sample, leads to the observed decrease of internal diffusion rate. By the same reason, the more acidic character of AC-P sample inhibits water adsorption and leads to an increase of intra-particle diffusion rate. Furthermore, examination of Table 4, shows that carbon AC-A has the highest intercept value, AC-P the least and AC an intermediate value. This observation, further support the above suggested explanation and pointed out the greater boundary layer effect in the sorption process onto AC-A sample.

3.4. Real wastewater treatment

The plain and modified activated carbons were used directly in fixed bed-columns for rotenone removal from a real wastewater sample, containing 39 mg L^{-1} of rotenone. To explore the effect of applied modifications on the adsorption capacity of activated carbon, the amounts of rotenone adsorbed onto AC-A and AC-P carbons are measured as a function of total added insecticide and compared to that obtained with plain carbon (Fig. 5). The amount of rotenone adsorbed during the breakthrough experiment is calculated using the following equation:

$$Q(mg\ g^{-1}) = \frac{\sum_{i=1}^{n}(C_0 - C_{i,res})V_i}{m} \quad (4)$$

where C_0 is the initial concentration before treatment, m the mass of carbon packed in the column, $C_{i,res}$ and V_i are the residual concentration of rotenone and the volume of the ith fraction.

It is seen that all investigated carbons adsorbed relatively an important amounts of rotenone, following the same trend found in the batch adsorption experiments (AC-A > AC > AC-P). Indeed, the

Table 4
Intraparticle diffusion constants for rotenone adsorption on plain and modified carbons.

Activated carbon	Initial concentration (mg L^{-1})	k_{ip} (mg g^{-1}min $^{-1/2}$)	C (mg g^{-1})	R^2
AC	100	6.17	34.22	0.989
	50	3.56	12.21	0.977
	25	1.72	7.48	0.989
AC-A	100	5.21	43.23	0.978
	50	3.36	14.37	0.989
	25	1.72	7.79	0.977
AC-P	100	7.19	26.08	0.974
	50	3.63	10.61	0.989
	25	2.08	5.22	0.987

rotenone uptakes of AC-A, AC and AC-P carbons were found to be 147.3 mg g^{-1}, 125 mg g^{-1} and 95 mg g^{-1}, respectively. The differences between adsorption capacities, found by batch type sorption experiments and fixed bed procedure, could be attributed to the competitive adsorption of organic and mineral species present in the rinsate effluent. Another alternative explanation that could be attributed to the applied flow rate and, as a consequence, to the contact time which was not sufficient to reach equilibrium and to have complete removal of rotenone.

The break-through curves presented in Fig. 5, showed that the column (2.5 g) of ammonia-impregnated carbon was effective in reducing more than 97% of rotenone concentration (from 39 to 1 mg L^{-1}) in 390 mL of the real effluent, while the plain carbon could be used with the same efficacy for the treatment of 200 mL of real wastewater.

4. Conclusion

The present work has demonstrated the essential role of surface chemistry on determining the adsorption capacity of rotenone on powdered activated carbon. It has been shown that rotenone uptake increased with the concentration of total surface bases and decreased upon increasing carboxylic groups, showing that the most important mechanism for the adsorption of rotenone on activated carbon involves pi-pi dispersive interactions. The equilibrium data followed the Langmuir isotherm with a maximum adsorption capacities reached 178.6, 217.4 and 270.3 mg g^{-1} for AC- P, AC and AC-A, respectively. The sorption kinetic data fitted the pseudo-second order model, while the Weber-Morris plot showed that intra-particle diffusion was not the only limiting step that governs the adsorption rate and that external diffusion (boundary layer diffusion) is also significant, especially at the initial reaction period. The successful application of activated carbons to the treatment of real wastewater sample, showed that adsorption of rotenone on plain or ammonia-treated AC could be considered as suitable alternative for the removal of this insecticide from contaminated wastewaters generated from applicator's container rinsates, agrochemical industries, formulation and manufacturing plants.

Acknowledgement

The authors would like to sincerely acknowledge Prof. Abdelhamid Ghorbel and Prof. Latifa Bergaoui for performing the BET measurements.

References

[1] S.J. Kalkhoff, D.W. Kolpin, E.M. Thurman, I. Ferrer, D. Barcelo, Degradation of Chloroacetanilide Herbicides: The Prevalence of Sulfonic and Oxanilic Acid Metabolites in Iowa Groundwaters and Surface Waters, Environ. Sci. Technol. 32 (1998) 1738–1740.
[2] Q. Wang, A.T. Lemley, Kinetic Model and Optimization of 2,4-D Degradation by Anodic Fenton Treatment, Environ. Sci. Technol. 35 (2001) 4509–4514.
[3] S. Chiron, A.R. Fernandez-Alba, A. Rodriguez, Pesticide chemical oxidation processes: an analytical approach, Trends Anal. Chem. 16 (9) (1997) 518–527.
[4] H.P. Boehm, Some aspects of the surface chemistry of carbon blacks and other carbons, Carbon 32 (1994) 759–769.
[5] T.J. Bandosz, Effect of pore structure and surface chemistry of virgin activated carbons on removal of hydrogen sulfide, Carbon 37 (1999) 483–491.
[6] A.R. Hind, S.K. Bhargava, S.C. Grocott, The surface chemistry of Bayer process solids: a review, Colloids Surf. A 146 (1999) 359–374.
[7] C.Y. Yin, M.K. Aroua, W.M.A.W. Daud, Review of modifications of activated carbon for enhancing contaminant uptakes from aqueous solutions, Sep. Purif. Technol. 52 (2007) 403–415.
[8] A. Dąbrowski, P. Podkościelny, Z. Hubicki, M. Barczak, Adsorption of phenolic compounds by activated carbon—a critical review, Chemosphere 58 (2005) 1049–1070.
[9] J.M. Dias, M.C.M. Alvim-Ferraz, M.F. Almeida, J. Rivera-Utrilla, M. Sánchez-Polo, Waste materials for activated carbon preparation and its use in aqueous-phase treatment: A review, J. Env. Management 85 (2007) 833–846.
[10] L. Monser, N. Adhoum, Modified activated carbon for the removal of copper, zinc, chromium and cyanide from wastewater, Sep, Purif. Technol. 26 (2002) 137–146.
[11] N. Adhoum, L. Monser, Removal of phthalate on modified activated carbon: application to the treatment of industrial wastewater, Sep. Purif. Technol. 38 (2004) 233–239.
[12] N. Adhoum, L. Monser, Removal of cyanide from aqueous solution using impregnated activated carbon, Chem. Eng. Process. 41 (2002) 17–21.
[13] K. Okawa, K. Suzuki, T. Takeshita, K. Nakano, Regeneration of granular activated carbon with adsorbed trichloroethylene using wet peroxide oxidation, Water Research 41 (2007) 1045–1051.
[14] C. Moreno-Castilla, Adsorption of organic molecules from aqueous solutions on carbon materials, Carbon 42 (2004) 83–94.
[15] M. Santiago, F. Stüber, A. Fortuny, A. Fabregat, J. Font, Modified activated carbons for catalytic wet air oxidation of phenol, Carbon 43 (2005) 2134–2145.
[16] P. Cañizares, M. Carmona, O. Baraza, A. Delgado, M.A. Rodrigo, Adsorption equilibrium of phenol onto chemically modified activated carbon F400, J. Hazard. Mater. 131 (2006) 243–248.
[17] J. Przepiórski, Enhanced adsorption of phenol from water by ammonia-treated activated carbon, J. Hazard. Mater. 135 (2006) 453–456.
[18] J. Alcañiz-Monge, M.J. Illán-Gómez, Insight into hydroxides-activated coals: Chemical or physical activation, J. Colloid Interface Sci. 318 (2008) 35–41.
[19] P. Pendleton, S.H. Wu, A. Badalyan, Activated carbon oxygen content influence on water and surfactant adsorption, J. colloid. Interface Sci. 246 (2002) 235–240.
[20] P. Pendleton, S.H. Wong, R. Schumann, G. Levay, R. Denoyel, J. Rouquerol, Properties of activated carbon controlling 2-Methylisoborneol adsorption, Carbon 35 (1997) 1141–1149.
[21] A.P. Terzyk, Further insights into the role of carbon surface functionalities in the mechanism of phenol adsorption, J. colloid. Interface Sci. 268 (2003) 301–329.
[22] V. Fierro, V. Torné-Fernández, D. Montané, A. Celzard, Adsorption of phenol onto activated carbons having different textural and surface properties, Micropor. Mesopor. Mater. 111 (2008) 276–284.
[23] J. Lee, M.-S. Huang, I.-C. Yang, T.-C. Lai, J.-L. Wang, V.F. Pang, M. Hsiao, M.Y.P. Kuo, Essential roles of caspases and their upstream regulators in rotenone-induced apoptosis, Biochem. Biophys. Res. Commun. 371 (2008) 33–38.
[24] K. Radad, W.-D. Rausch, G. Gille, Rotenone induces cell death in primary dopaminergic culture by increasing ROS production and inhibiting mitochondrial respiration, Neurochem. Intern. 49 (2006) 379–386.
[25] R. Betarbet, T.B. Sherer, G. MacKenzie, M. Garcia-Osuna, A.V. Panov, J.T. Greenamyre, Chronic systemic pesticide exposure reproduces features of Parkinson's disease, Nat. Neurosci. 3 (2000) 1301–1306.
[26] B. Latli, E. Wood, J.E. Casida, Insecticidal quinazoline derivatives with (trifluoromethyl)diazirinyl and azido substituents as NADH:ubiquinone oxidoreductase inhibitors and candidate photoaffinity probes, Chem. Res. Toxicol. 9 (1996) 445–450.
[27] N. Li, K. Ragheb, G. Lawler, J. Sturgis, B. Rajwa, J.A. Melendez, J.P. Robinson, Mitochondrial complex I inhibitor rotenone induces apoptosis through enhancing mitochondrial reactive oxygen species production, J. Biol. Chem. 278 (2002) 8516–8525.
[28] S. Tada-Oikawa, Y. Hiraku, M. Kawanishi, S. Kawanishi, Mechanisms of generation of hydrogen peroxide and change of mitochondrial membrane potential during rotenone-induced apoptosis, Life Sci. 73 (2003) 3277–3288.
[29] W.G. Chung, C.L. Miranda, C.S. Maier, Epigallocatechin gallate (EGCG) potentiates the cytotoxicity of rotenone in neuroblastoma SH-SY5Y cells, Brain Res. 1176 (2007) 133–142.
[30] G.U. Höglinger, Chronic systemic complex I inhibition induces a hypokinetic multisystemdegeneration in rats, J. Neurochem. 84 (2003) 1–12.
[31] T.B. Sherer, J.H. Kim, R. Betarbet, J.T. Greenamyre, Subcutaneous rotenone exposure causes highly selective dopaminergic degeneration and alphasynuclein aggregation, Exp. Neurol. 179 (2003) 9–16.
[32] T.B. Sherer, R. Betarbet, A.K. Stout, S. Lund, M. Baptista, A.V. Panov, M.R. Cookson, J.T. Greenamyre, An in vitro model of Parkinson's disease: linking mitochondrial impairment to altered alpha-synuclein metabolism and oxidative damage, J. Neurosci. 22 (2002) 7006–7015.
[33] Y. Ren, J. Feng, Rotenone selectively kills serotonergic neurons through a microtubule-dependent mechanism, J. Neurochem. 103 (2007) 303–311.
[34] I. Cavoski, P. Caboni, G. Sarais, P. Cabras, T. Miano, Photodegradation of Rotenone in Soils under Environmental Conditions, J. Agric. Food Chem. 55 (2007) 7069–7074.
[35] W.M. Draper, Near UV quantum yields for rotenone and piperonyl butoxide, Analyst 127 (2002) 1370–1374.
[36] H.M. Cheng, I. Yomamoto, J. Casida, Rotenone photodecomposition, J. Agric. Food Chem. 20 (1972) 850–855.
[37] M. Tennant, D. Mazyck, Steam-pyrolysis activation of wood char for superior odorant removal, Carbon 41 (8) (2003) 2195–2202.
[38] O.B. Samuelsen, E. Solheim, H. Oterra, J.P. Pedersen, The toxicity, absorption and excretion of rotenone in oysters (Ostrea edulis), and its degradation in seawater at temperatures near 0 °C, Aquaculture 70 (1988) 355–363.
[39] S.S Barton, M.J.B. Evans, E. Halliop, J.A.F. Mac Donald, Acidic and basic sites on the surface of porous carbon, Carbon 35 (1997) 1361–1366.
[40] B.M. Babić, S.K. Milonjić, M.J. Polovina, B.V. Kaludierović, Point of zero charge and intrinsic equilibrium constants of activated carbon cloth, Carbon 37 (1999) 477–481.
[41] S.K. Milonjić, A.L. Ruvarac, M.V. Šušić, The heat of immersion of natural magnetite in aqueous solutions, Thermochim. Acta 11 (3) (1975) 261–266.

[42] G. Newcombe, R. Hayes, M. Drikas, Granular activated carbon: Importance of surface properties in the adsorption of naturally occurring organics, Colloids Surf. A 78 (1993) 65–71.
[43] S. Biniak, G. Szymański, J. Siedlewski, A. Swiatkoski, The characterization of activated carbons with oxygen and nitrogen surface groups, Carbon 35 (1997) 1799–1810.
[44] M.A. Montes-Morán, D. Suárez, J.A. Menéndez, E. Fuente, On the nature of basic sites on carbon surfaces: An overview, Carbon 42 (2004) 1219–1224.
[45] P. Chingombe, B. Saha, R.J. Wakeman, Effect of surface modification of an engineered activated carbon on the sorption of 2,4-dichlorophenoxy acetic acid and benazolin from water, J. Colloid. Interface Sci. 297 (2006) 434–442.
[46] B.H. Hameed, I.A.W. Tan, A.L. Ahmad, Adsorption isotherm, kinetic modeling and mechanism of 2,4,6-trichlorophenol on coconut husk-based activated carbon, Chem. Eng. J. 144 (2008) 235–244.
[47] S. Haydar, M.A. Ferro-García, J. Rivera-Utrilla, J.P. Joly, Adsorption of p-nitrophenol on an activated carbon with different oxidations, Carbon 41 (2003) 387–395.
[48] L.R. Radovic, C. Moreno-Castilla, J. Rivera-Utrilla, Carbon materials as adsorbents in aqueous solutions, in: L.R. Radovic (Ed.), Chemistry and physics of carbon, vol.27, Marcel Dekker, New York, 2000, pp. 227–405.
[49] D.M. Nevskaia, A. Santianes, V. Muñoz, A. Guerrero-Ruiĭz, Interaction of aqueous solutions of phenol with commercial activated carbons: An adsorption and kinetic study, Carbon 37 (1999) 1065–1074.
[50] M. Franz, H.A. Arafat, N.G. Pinto, Effect of chemical heterogeneity on the adsorption mechanism of dissolved aromatics on activated carbon, Carbon 38 (2000) 1807–1819.
[51] W.J. Weber, J.C. Morris, Proc. Int. Conf. Water pollution symposium, vol.2, Pergamon, Oxford, 1962, pp. 231-266.
[52] F. Villacañas, M.F.R. Pereira, J.J.M. Órfão, J.L. Figueiredo, Adsorption of simple aromatic compounds on activated carbons, J. Colloid Interface Sci. 293 (2006) 128–136.
[53] L. Li, P.A. Quinlivan, D.R.U. Knappe, Effects of activated carbon surface chemistry and pore structure on the adsorption of organic contaminants from aqueous solution, Carbon 40 (2002) 2085–2100.